Response to "Comment on 'Finding finite-time invariant manifolds in two-dimensional velocity fields' " [Chaos 11, 427 (2001)]

G. Haller
Division of Applied Mathematics, Lefschetz Center for Dynamical Systems, Brown University, Providence, Rhode Island 02912

(Received 22 December 2000; accepted 2 April 2001; published 29 May 2001)

Lapeyre, Hua, and Legras have recently suggested that the detection of finite-time invariant manifolds in two-dimensional fluid flows, as described by Haller and Haller and Yuan, can be substantially improved. In particular, they suggested (a) a change of coordinates to strain basis before the application of Theorem 1 of Haller and (b) the use of a nondimensionalized time computed from Theorem 1. Here we discuss why these proposed steps will *not* result in a significant overall improvement. We verify our arguments in a more detailed computation of the example analyzed in Lapeyre, Hau, and Legras (the Kida ellipse), as well as in a two-dimensional barotropic turbulence simulation. While in both of these examples the techniques suggested by Lapeyre, Hau, and Legras reveal additional thin regions of hyperbolicity near vortex cores, they also lead to an overall loss of detail in the global computation of finite-time invariant manifolds. [DOI: 10.1063/1.1374242]

Recent results have shown that mixing in two-dimensional velocity fields with general time dependence is governed by finite-time stable and unstable manifolds. Haller proved a theorem on the existence of such structures in general velocity fields. In a commentary on this theorem, Lapeyre, Hua and Legras have suggested that changing coordinates before the application of the main theorem of Haller would lead to a significant improvement in the detection of finite-time invariant manifolds. They also proposed the strain rate as a general indicator of such manifolds. In this paper we discuss why these suggestions will, in general, not lead to significant improvements. We illustrate our arguments through detailed computations of finite-time invariant manifolds in two examples.

I. SUMMARY OF THE MAIN RESULTS OF HALLER AND HALLER AND YUAN

In this section we recall the incompressible formulation of the main theorem in Haller (H), as stated in Haller and Yuan (HY), for two reasons. First, we need a precise statement of the results for our later arguments. Secondly, Lapeyre, Hua, and Legras (LHL) do not explicitly list our main theorem, and hence the reader may find it helpful to see a precise statement of the result in question.

A. General formulation

Consider a two-dimensional (2D) velocity field

$$\dot{\mathbf{x}}=\mathbf{u}(\mathbf{x},t), \quad \nabla\cdot\mathbf{u}=0, \tag{1}$$

where $\mathbf{u}$ is assumed to be smooth and given on a finite time interval $\mathcal{I}$. Suppose that a trajectory $\mathbf{x}(t)$ generated by this velocity field is known. The Jacobian of the velocity field along $\mathbf{x}(t)$ is then given by the time-dependent matrix $\nabla\mathbf{u}(\mathbf{x}(t),t)$, where ∇ denotes differentiation with respect to $\mathbf{x}$. We assume that on a closed time interval $I_u\subset\mathcal{I}$, the relation $\det\nabla\mathbf{u}(\mathbf{x}(t),t)<0$ holds, i.e., $\nabla\mathbf{u}(\mathbf{x}(t),t)$ has real eigenvalues $-\lambda(t)<0<\lambda(t)$. Let $\mathbf{e}_1(t)$ and $\mathbf{e}_2(t)$ denote the unit eigenvectors corresponding to $-\lambda(t)$ and $\lambda(t)$, selected in a way so that they vary smoothly in t. Introducing the matrix of eigenvectors, $\mathbf{T}(t)=[\mathbf{e}_1(t),\mathbf{e}_2(t)]$, we can then define the following three quantities:

$$\lambda_{\min}=\min_{t\in I_u}\lambda(t), \quad \alpha=\min_{t\in I_u}|\det\mathbf{T}(t)|, \quad \beta=\max_{t\in I_u]}|\dot{\mathbf{T}}(t)|. \tag{2}$$

Note that α is never zero by definition.

Theorem 1. *Suppose that for a fluid trajectory* $\mathbf{x}(t)$ *of the velocity field* (1) *we have, for all* $t\in I_u$,

$$\det\nabla\mathbf{u}(\mathbf{x}(t),t)<0, \quad \lambda_{\min}>(2+\sqrt{2})\frac{\beta}{\alpha}. \tag{3}$$

Then $\mathbf{x}(t)$ *is contained in a repelling material line over the time interval* I_u.

By a repelling material line we mean a material line that is linearly unstable throughout the time interval I_u, i.e., infinitesimal perturbations normal to it grow strictly monotonically within any subinterval of I_u. In dynamical systems terms, a repelling material line can be viewed as a two-dimensional finite-time stable manifold to a fluid trajectory in the extended phase space of the $(\mathbf{x},t)$ variables (see H). Attracting material lines (finite-time unstable manifolds) can be defined as material lines that are repelling in backward time.

We finally note that the two inequalities in (3) are fully equivalent to the five conditions listed in Eqs. (6) and (7) of H when those are restricted to incompressible flows. Since the commentary of LHL considers an incompressible example, we will stay with our discussion in that framework for simplicity. Also, we will follow the more compact (but otherwise equivalent) notation developed in HY.

B. Lagrangian coherent structures (LCS)

1. Definition of LCS

As proposed in H and discussed in detail in HY, *Lagrangian coherent structures* (LCS) in a turbulent flow can be defined as material lines that are attracting or repelling for locally the longest time in the flow. More specifically, repelling LCS will be material lines that evolve from the local maximizing curves of the scalar field

$$T_u(\mathbf{x}_0,t_0)=\int_{\cup I_u(\mathbf{x}_0,t_0)} dt,$$

where $\cup I_u(\mathbf{x}_0,t_0)$ refers to the union of all subintervals within $\mathcal{I}$ over which the trajectory starting from $\mathbf{x}_0$ at time t_0 satisfies both conditions in (3). Similarly, attracting Lagrangian coherent structures (finite-time unstable manifolds) will be material lines evolving from the local maximizers of a scalar field $T_s(\mathbf{x}_0,t_0)$ that measures the time that a trajectory spends in attracting material lines.

2. Theorem 1 and LCS

The significance of Theorem 1 is that it gives a lower bound for $T_u(\mathbf{x}_0,t_0)$: This bound is the total length of time within $\mathcal{I}$ over which (3) are satisfied. Applying the theorem in backward time yields a lower bound for $T_s(\mathbf{x}_0,t_0)$. It then remains to plot these two fields and extract their local maximizing curves. It turns out that instead of simply focusing on maximizing curves, one should generally look for local extremum curves of $T_s(\mathbf{x}_0,t_0)$ and $T_u(\mathbf{x}_0,t_0)$, including local *minimizing* curves. LCS associated with local minimizing curves will occur in flows with no-slip boundary conditions (cf. HY).

3. Numerical detection of LCS

In practice, one checks the conditions of Theorem 1 for a grid of initial conditions launched at $t=t_0$ to obtain the discrete scalar fields $T_u(\mathbf{x}_0^{i,j},t_0)$ and $T_s(\mathbf{x}_0^{i,j},t_0)$. The Lagrangian coherent structures detected in this fashion will be the ones that admit a separation of Eulerian and Lagrangian time scales: The second condition in (3) requires Lagrangian particle speeds to dominate Eulerian deformation rates. Fast-rotating eddies may violate this condition, in which case their Lagrangian boundaries will not be fully detected by the above procedure: parts of their bounding material lines come out hazy or completely lost in the plots of $T_u(\mathbf{x}_0^{i,j},t_0)$ and $T_s(\mathbf{x}_0^{i,j},t_0)$. Nevertheless, the numerical study of HY suggests that most coherent structures in 2D turbulence admit a sufficient separation of Eulerian and Lagrangian time scales that renders them visible to the above analysis. It appears that one could even take such a time scale separation as a defining property of robust coherent structures.

4. Extracting stronger LCS

If one's interest is specifically to recover *strongly* repelling or attracting LCS in the flow, a systematic filtering of material lines with weaker hyperbolicity is possible as follows:

(i) When calculating $T_u(\mathbf{x}_0,t_0)$, one can simply set a positive threshold λ_0 for admissible $\lambda_{\min}$ values before even verifying (3). This amounts to calculating the scalar field

$$T_u(\mathbf{x}_0,t_0,\lambda_0)=\int_{\substack{\cup I_u(\mathbf{x}_0,t_0)\\ \lambda_{\min}\geqslant\lambda_0}} dt. \tag{4}$$

This is actually *not* an *ad hoc* technique: it is proved in H that the strength of hyperbolicity for structures detected by Theorem 1 is of the order of $\lambda_{\min}-\mathcal{O}(\beta/\alpha)$. Therefore, one can justifiably increase the admissible $\lambda_{\min}$ in the calculation to filter out weaker LCS gradually. For an application of this procedure, see HY.

(ii) A further refinement is obtained from a closer inspection of the proof of Theorem 1 [see H, Eq. (21)]. The proof reveals that the type of repelling LCS captured by the theorem repel nearby particles at an exponential rate with the approximate exponent $\int_{t_0}^{t}\lambda(\tau)d\tau$. Plotting, therefore, the field

$$l_u(\mathbf{x}_0,t_0,\lambda_0)=\int_{\substack{\cup I_u(\mathbf{x}_0,t_0)\\ \lambda_{\min}\geqslant\lambda_0}} \lambda(t)dt, \tag{5}$$

instead of $T_u(\mathbf{x}_0,t_0)$ will further enhance the visibility of strongly repelling LCS.

While these two techniques can be useful in a better visualization of the structures obtained from Theorem 1, they will also suppress other structures with weaker hyperbolicity.

II. THE MAIN POINTS OF THE LAPEYRE–HUA–LEGRAS COMMENTARY

Lapeyre, Hua, and Legras propose two ways to improve the applicability of Theorem 1 in Haller, or equivalently, its incompressible counterpart, Theorem 1 of this note.

A. Change of frame

First, LHL propose to transform the velocity field $\mathbf{u}(\mathbf{x},t)$ to a different frame along the trajectory $\mathbf{x}(t)$ before the application of Theorem 1. The coordinate system they suggest is defined by the eigenvectors of the matrix

$$\mathbf{S}(t)=\tfrac{1}{2}(\nabla\mathbf{u}(\mathbf{x}(t),t)+(\nabla\mathbf{u}(\mathbf{x}(t),t))^T),$$

which is just the rate-of-strain tensor evaluated along the trajectory $\mathbf{x}(t)$. Denoting the matrix of normalized rate-of-strain eigenvectors by $\mathbf{R}(t)$ and using the fact that $\mathbf{R}^{-1}=\mathbf{R}^T$, the transformation can be written as

$$\mathbf{y}=\mathbf{R}^T(t)(\mathbf{x}-\mathbf{x}(t)). \tag{6}$$

In the transformed set of coordinates the underlying trajectory $\mathbf{x}(t)$ satisfies $\mathbf{y}\equiv\mathbf{0}$, and the gradient of the transformed velocity field $\dot{\mathbf{y}}=\tilde{\mathbf{u}}(\mathbf{y},t)$ can be written along it as

$$\nabla\tilde{\mathbf{u}}(\mathbf{0},t)=\mathbf{R}^T(t)\nabla\mathbf{u}(\mathbf{x}(t),t)\mathbf{R}(t)-\mathbf{R}^T(t)\dot{\mathbf{R}}(t). \tag{7}$$

Since the columns of $\mathbf{R}(t)$ are unit vectors for all t, they are orthogonal to the corresponding columns of $\dot{\mathbf{R}}(t)$. As a result, $\mathbf{R}^T\dot{\mathbf{R}}$ is a skew-symmetric matrix with zero diagonal elements. This in turn implies that $\nabla\tilde{\mathbf{u}}$ has zero trace, i.e., $\tilde{\mathbf{u}}$ is incompressible with respect to the variable $\mathbf{y}$. Consequently, one can use Theorem 1 to check the finite-time hyperbolicity of the $\mathbf{y}=\mathbf{0}$ trajectory.

As LHL point out, one can in principle pick any time-dependent proper orthogonal matrix $\mathbf{R}$, compute the gradient $\nabla\tilde{\mathbf{u}}$ in the new basis and apply Theorem 1 to the transformed equation. While the theorem is Galilean invariant, it is not invariant under rotations by matrices $\mathbf{R(t)}$ that very *fast enough* in time (cf. H). As a result, if the eigenvectors of $\mathbf{S}(t)$ rotate fast enough in time, the theorem may guarantee hyperbolicity in the new coordinates but not in the old ones or vice versa. LHL believe that this is typically the case and declare the above change of coordinates before the application of Theorem 1 a ''substantial improvement'' on the theorem.

B. Use of strain rate

The second suggestion of LHL concerns the definition and visualization of Lagrangian coherent structures: Instead of identifying Lagrangian coherent structures as extrema of $T_u(\mathbf{x}_0,t_0)$ and $T_s(\mathbf{x}_0,t_0)$, they seek them as local extrema of the strain rate $\sigma(\mathbf{x}(t),t)$ integrated over periods of instability/stability detected along the trajectory $\mathbf{x}(t)$. In terms of the components of the transformed velocity field $\tilde{\mathbf{u}}=(u,v)$, the strain rate σ is defined as

$$\sigma=\sqrt{\sigma_n^2+\sigma_s^2},\quad \sigma_n=\partial_x u-\partial_y v,\quad \sigma_s=\partial_x v+\partial_y u,$$

and the integrated strain rate is

$$e(\mathbf{x}_0,t_0)=\int_{\cup\tilde{I}_u(\mathbf{x}_0,t_0)}\sigma(\mathbf{x}(t),t)\,dt.$$

Here $\cup\tilde{I}_u(\mathbf{x}_0,t_0)$ refers to the union of all subintervals within $\mathcal{I}$ over which the trajectory starting from $\mathbf{x}_0$ at time t_0 satisfies both conditions in (3) computed in strain basis.

III. ARE THESE IMPROVEMENTS?

Based on the analysis presented below, they are *not*. We shall give reasons why one should typically get similar or somewhat weaker results after implementing the suggestions of LHL. In Sec. IV we illustrate this by recomputing *both* conditions of Theorem 1 in strain basis as well as in the original basis, a task that LHL did not perform (cf. Sec. III of LHL). In Sec. V we also compare the two approaches on the barotropic turbulence simulation of HY. In both numerical experiments the results will confirm the arguments given below.

A. Change of frame

The main point of Haller was the proof of the general compressible version of Theorem 1. In that paper we considered a single example in which we only verified the first condition of Theorem 1 for illustration. However, we also warned that this ''first approximation'' would not suffice for more complicated flows: The intervals $\cup I_u(\mathbf{x}_0,t_0)$ must be determined by verifying both conditions given in (3). (This more complete implementation was discussed and tested in HY.)

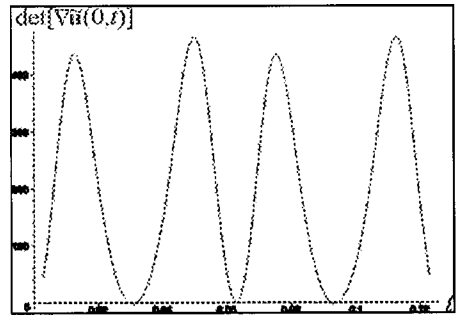

FIG. 1. The quantity det $\nabla\tilde{\mathbf{u}}(0,t)$ for the example velocity field (8), shown over two periods of the function $a(t)$.

LHL appear to have overlooked this warning and based their modification on the first condition only and not the full theorem. Regarding the first condition, it is certainly true that it may not be satisfied in the original frame while it is satisfied in the strain basis, a point that LHL emphasize with their example of the Kida ellipse. However, this can just as well happen the other way around, too. Consider, e.g., the incompressible velocity field

$$\mathbf{u}(\mathbf{x},t)=\begin{pmatrix}1 & a(t)\\ 0 & -1\end{pmatrix}\mathbf{x},\tag{8}$$

for which $\mathbf{x}=\mathbf{0}$ is a uniformly hyperbolic fixed point (as seen by direct integration) and hence is contained in the repelling material line $\{x_2\equiv 0\}$ (finite-time stable manifold) over any finite time interval. The first condition of Theorem 1 is trivially satisfied for *all times* along $\mathbf{x}=\mathbf{0}$. Passing to strain basis, this will not necessarily be the case. For instance, picking $a(t)=2\sin^2(50t)$, a uniformly bounded function with fast oscillations, can produce a strain basis in which $\det[\nabla\tilde{\mathbf{u}}(\mathbf{0},t)]$ is predominantly positive (see Fig. 1). Since the rare negative determinant values are very small in norm, one would normally discount them in a numerical calculation as errors, and conclude that the origin is not hyperbolic (in strain basis).

As for the second condition of Theorem 1, it essentially requires that the rotation rate β of the eigenvectors of $\nabla\mathbf{u}(\mathbf{x}(t),t)$ be small compared to the norm of its eigenvalues. For a typical fluid trajectory, the eigenvectors of $\mathbf{S}(t)$ rotate at a similar speed, and hence the term $\mathbf{R}^T(t)\dot{\mathbf{R}}(t)$ will also be of $\mathcal{O}(\beta)$. For Theorem 1 to apply to this trajectory in strain basis, the rotation speed of the eigenvectors of $\nabla\tilde{\mathbf{u}}(\mathbf{0},t)$, again of order $\mathcal{O}(\beta)$, must be small compared to the norm of its eigenvalues. Since $\mathbf{R}^T(t)\dot{\mathbf{R}}(t)$ is of order $\mathcal{O}(\beta)$, the eigenvalues of $\nabla\tilde{\mathbf{u}}(\mathbf{0},t)$ are $\mathcal{O}(\beta)$-close to those of $\mathbf{R}^T(t)\nabla\mathbf{u}(\mathbf{x}(t),t)\mathbf{R}(t)$, or equivalently, to those of $\nabla\mathbf{u}(\mathbf{x}(t),t)$. Therefore, in strain basis the second condition of Theorem 1 will be of the type

$$\lambda_{\min}+\mathcal{O}(\beta)>\mathcal{O}(\beta),$$

where β and $\lambda_{\min}$ are computed in the *original* basis. In general, this condition requires the same order of separation between Eulerian and Lagrangian time scales as the second condition in (3). Therefore, for fluid trajectories launched from a generic initial grid, one should not expect a major improvement from passing to strain basis in the calculation.

The above argument applies to generic fluid trajectories. In a given problem with special symmetries or special time scales one *may* get different results using Theorem 1 in the ''lab frame'' or rotating frame. In certain regions of the flow the lab frame may give a somewhat sharper result, while in other regions the strain frame or some other frame may prevail as a better choice.

From a computational point of view, however, it does not seem to be efficient to experiment with all possible choices of frame for a more complex velocity field. Performing the time-dependent change of coordinates (6) along each trajectory for all times does increase computation time and introduces further numerical errors. In particular, to obtain β in strain basis, one has to differentiate the components of $\nabla\tilde{\mathbf{u}}$ in time. These components already contain time derivatives, so one ends up taking second derivatives in time.

In summary, passing to a strain basis, as suggested by LHL, should not lead to major improvements in the application of Theorem 1 for most velocity fields. However, it may lead to additional numerical errors that affect the analysis. We shall illustrate this in Secs. IV and V.

B. Use of strain rate

As LHL say, the introduction of the strain rate is a heuristic way to improve the extraction of Lagrangian coherent structures. They expect the scalar field $e(\mathbf{x}_0,t_0)$ to admit maxima along repelling material lines that are sharper than those of the instability time field $T_u(\mathbf{x}_0,t_0)$.

This is certainly a reasonable expectation for strongly repelling material lines, and hence the use of the strain rate will indeed increase the visibility of the strongest Lagrangian coherent structures while suppressing weaker ones. However, such a systematic filtering can be more efficiently achieved by (a) raising the admissible hyperbolicity threshold $\lambda_{\min}$ in the calculation (b) and/or plotting the integral of $\lambda(t)$, which gives an approximation of the true Lagrangian stretching rate (cf. Sec. I B 4). The error in this approximation is known to be $\mathcal{O}(\beta/\alpha)$, which is small compared to $\lambda(t)$ since otherwise Theorem 1 would not apply to begin with. Also, changing the hyperbolicity threshold gives a smooth and gradual way of filtering out weaker LCS.

In summary, the heuristic use of the field $e(\mathbf{x}_0,t_0)$ may improve the visibility of the strongest LCS while it suppresses weaker ones. At the same time, the non-heuristic use of a hyperbolicity threshold in the calculation of T_u, as suggested in HY, allows a localization of LCS at all levels of strength.

Again, we illustrate this point on examples in the forthcoming two sections.

IV. COMPARISON ON THE KIDA ELLIPSE

A. Change of frame

To check the claim that passing to strain basis substantially improves the applicability of Theorem 1, we verified *both* conditions (3) in the ''lab frame'' as well as in strain basis. We performed the calculations both on the time interval [0,2] chosen by LHL, as well as on the longer interval [0,4]. Just as LHL, we restricted ourselves to forward-time calculations, aiming to locate repelling LCS (finite-time stable manifolds). As an independent point of reference, we first employed a Direct Lyapunov Exponent (DLE) calculation that identifies LCS as local extrema of the deformation gradient field [see Haller (H3D) for details]. The results of these calculations are shown in Figs. 2(a) and 2(d). Below these pictures we present the plots of $T_u(\mathbf{x}_0,0)$ in the original frame [Figs. 2(b) and 2(e)] as well as in the strain basis proposed by LHL [Figs. 2(c) and 2(f)]. As we indicated earlier, we have not been able to find any overall ''substantial'' improvement: parts of the plots are more visible in strain basis (note the structures near the core of the vortex), while other parts in the original basis. In either basis, the main LCS is fairly well identified by Theorem 1, and is in agreement with the more detailed structure obtained from the DLE calculation. (For a discussion on the shortcomings of the DLE calculation, see Haller (H3D).]

B. Use of strain rate

To evaluate the use of integrated strain rate plots as opposed to hyperbolicity time plots, we repeated the above calculations with the same parameter values. Here we only show the results for the [0,4] time interval as the differences among different techniques become more visible on this longer interval.

In Fig. 3(a) we show the implementation of both techniques proposed by LHL: We plot the $e(\mathbf{x}_0,0)$ field based on the evaluation of Theorem 1 in strain basis. As we discussed in Sec. III B, one expects similar or better identification of LCS by implementing the two filtering techniques described in Sec. I B 4. Figures 3(b)–3(d) indeed confirm this. In particular, Fig. 3(b) shows the plot of the hyperbolicity time field $T_u(\mathbf{x}_0,0,1.5)$ [cf. formula (4)], while Figs. 3(c) and 3(d) show the fields $l_u(\mathbf{x}_0,0,1.5)$ and $l_u(\mathbf{x}_0,0,2.5)$, respectively [cf. formula (5)]. Again, as the pictures show, we have been unable to detect any ''substantial'' improvement resulting from the implementation of the suggestions of LHL. In fact, Fig. 3(a) shows *weaker* results than the others. Also note that the local advantage of the LHL algorithm near vortex cores disappears if one employs the λ-filtering of Sec. I B 4: The results shown in Fig. 3(c) are sharper both near the vortex cores as well as away from them.

V. COMPARISON ON 2D BAROTROPIC TURBULENCE

In order to test our arguments given in Sec. III further, we also examined the spatially and temporally more complex problem of two-dimensional barotropic turbulence. We reconsidered the simulation already studied in HY and implemented both suggestions of LHL in the calculation.

The velocity field was generated by the barotropic turbulence solver of A. Provenzale (for more details and references, see HY). The flow is doubly periodic on the spatial domain $[0,2\pi]^2$, and the velocity field we considered was given on the time interval [50,99]. (The simulation started

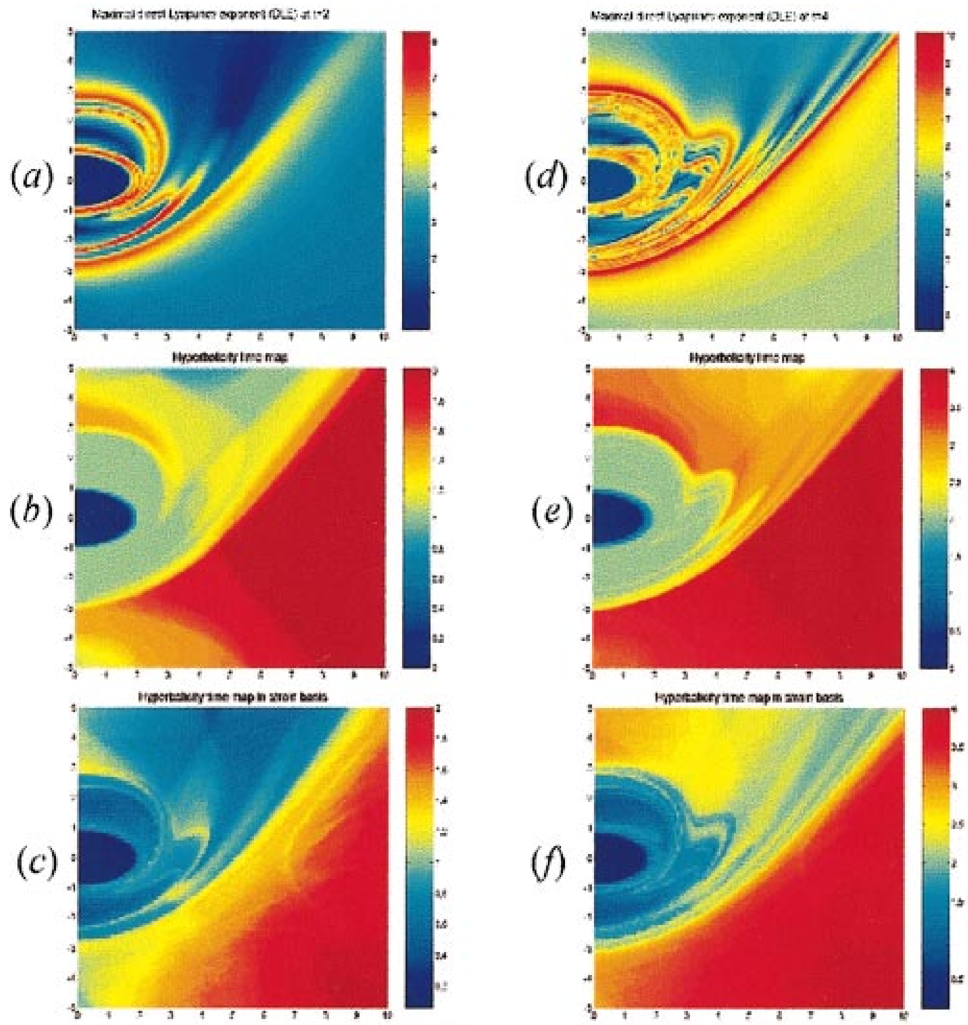

FIG. 2. (Color) Computation of repelling LCS at $t=0$ in the spatial domain $[0,10]\times[-5,5]$ using different methods: (a) DLE up to $t=2$; (b) hyperbolicity map up to $t=2$; (c) hyperbolicity map in strain basis up to $t=2$; (d) DLE up to $t=4$; (e) hyperbolicity map at $t=4$; (f) hyperbolicity map in strain basis at $t=4$.

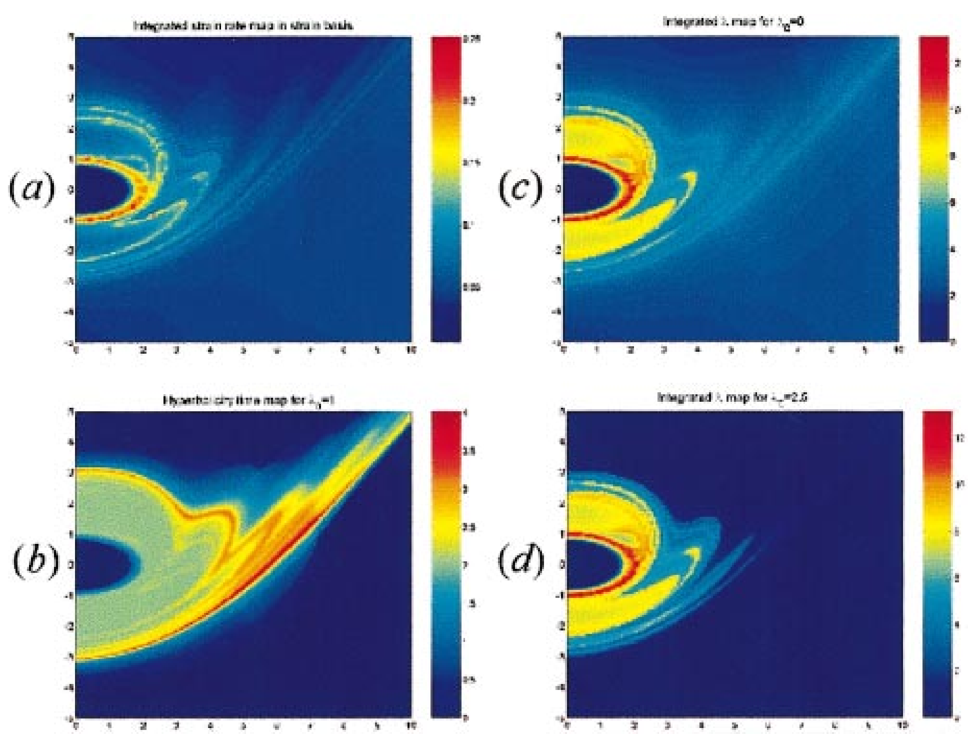

FIG. 3. (Color) Further comparison of repelling LCS for the Kida ellipse using different methods: (a) Implementation of both improvements proposed by LHL (strain basis+use of strain rate); (b) hyperbolicity map for $\lambda_{\min} > 1.5$, i.e., the $T_u(\mathbf{x}_0,0,1.5)$ field; (c) integration of $\lambda(\tau)$ for $\lambda_{\min} \geqslant 1.5$, i.e., the $l_u(\mathbf{x}_0,0,1.5)$ field; (d) integration of $\lambda(\tau)$ for $\lambda_{\min} \geqslant 2.5$, i.e., the $l_u(\mathbf{x}_0,0,2.5)$ field.

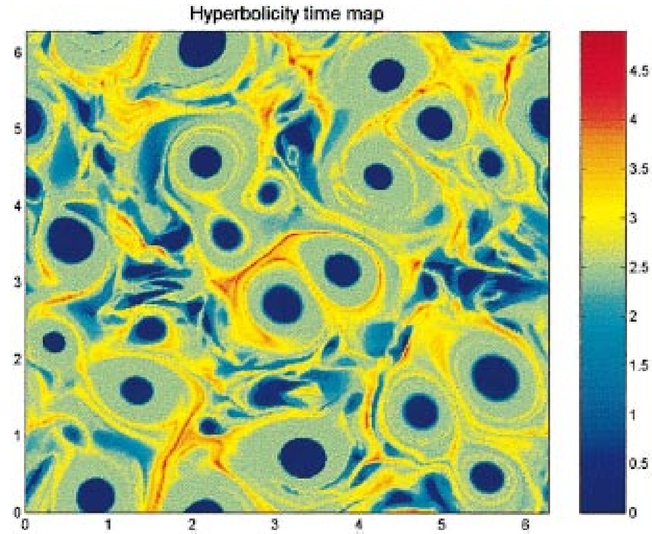

FIG. 4. (Color) Hyperbolicity time plot for two-dimensional barotropic turbulence.

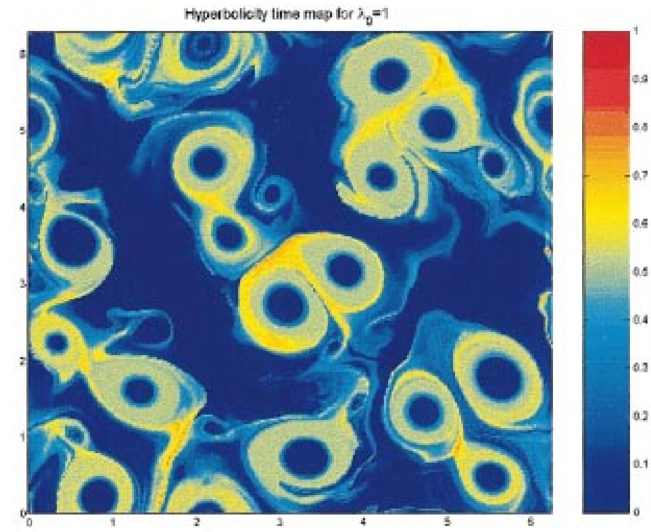

FIG. 6. (Color) Same as in Fig. 4, but with hyperbolicity threshold $\lambda_0 = 1$.

with Gaussian vorticity distribution at $t=0$. We started our LCS analysis at $t=50$, by which time robust coherent structures had already formed.)

In Fig. 4 we show the hyperbolicity time field $T_u(\mathbf{x}_0,50)$, reproduced from HY. In contrast, Fig. 5 shows the plot of the field $e(\mathbf{x}_0,50)$ suggested by LHL. In this comparison a ''substantial improvement'' is even more difficult to claim: The $e(\mathbf{x}_0,50)$ is fairly noisy and misses details of several LCS in background turbulence. It does provide an ''edge detection'' of the strongest structures, but a smoother and mathematically more rigorous filtering of hyperbolicity can be obtained from the use of the $T_u(\mathbf{x}_0,50,1.5)$ field, whose plot we reproduce in Fig. 6. Again, the advantage of using $T_u(\mathbf{x}_0,50,\lambda_0)$ is that one can ''sweep through'' coherent structures of different strength by varying λ_0 continuously. The only advantage of following the suggestions of LHL appears to be the fact that Fig. 5 indicates rings of high hyperbolicity around vortex cores, as noted by Lapeyre (L).

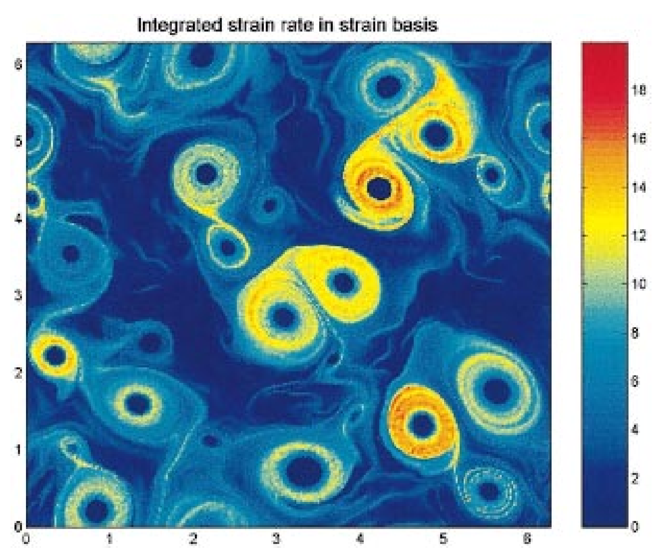

FIG. 5. (Color) The plot of the $e_u(\mathbf{x}_0,50)$ field, proposed by Lapeyre, Hua, and Legras, for the turbulent velocity field analyzed in Fig. 4.

VI. CONCLUSIONS

In this note we examined two recently proposed techniques by LHL, who have announced improvements of the main theorem of H for the extraction of finite-time Lagrangian coherent structures from unsteady 2D velocity fields. The proposal of LHL involves (a) passing to a basis defined by the time-dependent eigenvectors of the rate of strain tensor *before* the application of Theorem 1 of H (or, equivalently, Theorem 1 of HY for incompressible flows) and (b) identifying Lagrangian coherent structures as extrema of the integral of strain rate, as opposed to the hyperbolicity time field.

We gave arguments as to why the above two steps will, in general, not yield any improvements over the direct application of the results of H and HY. On the contrary, the numerically sensitive computation proposed in (a) and the *ad hoc* diagnostic tool suggested in (b) may in fact lead to weaker results in the numerical implementation of Theorem 1.

We illustrated our arguments on two examples. First, we recomputed the Kida ellipse problem considered by LHL with and without their proposed improvements. A main difference in our calculation is that we *fully* implemented Theorem 1 as opposed to the partial implementation of LHL. In agreement with our arguments, we have not seen any overall improvement in the results.

As a second example, we considered a numerically more challenging example, the velocity field obtained from a two-dimensional barotropic turbulence simulation. For this problem the scheme proposed by LHL performed noticeably weaker than a straight implementation of Theorem 1.

Based on all the above, we have not found any evidence that would support a ''substantial,'' or as a matter of fact, *any* overall improvement over our results. We rush to add that there may be special flows for which a preliminary change of coordinates to strain basis (or some other frame) would yield benefits that supersede the numerical errors introduced in the process. We also acknowledge that certain details of coherent structures (such as hyperbolic strips near vortex cores) may be better visible in strain basis for a typical fluid flow—while other details are better visible in the lab frame or in some other frame. However, the overall quality of the results will not change, a fact that is due to the very nature of the conditions of Theorem 1: A significant change in the validity of the first condition will only occur in frames that rotate fairly fast, but such frames will typically also violate the second condition of the theorem (cf. Sec. III A).

No doubt that future improvements on Theorem 1 may in fact perform better in the basis of strain eigenvectors or in some other basis. There is certainly room and need for such improvements: One would ideally like to have a verifiable sufficient *and necessary* condition for finite-time hyperbolicity as opposed to the mere sufficient criterion provided by Theorem 1. An ideal criterion would actually be fully frame-independent (physically *objective*, not just Galilean invariant)—thereby eliminating any possible debate about the best choice of frame for its application.

ACKNOWLEDGMENTS

I would like to thank Guillaume Lapeyre for kindly making the routine generating the velocity field of the Kida ellipse available to me, as well as for his comments on this work. I would also like to thank Antonello Provenzale for his permission to use his turbulence solver. This work was partially supported by NSF Grant No. DMS-98-00922 and AFOSR Grant No. F49620-00-1-0133.

Haller, G., ''Finding finite-time invariant manifolds in two-dimensional velocity fields,'' Chaos **10**, 99–108 (2000).
Haller, G., ''Distinguished material surfaces and coherent structures in 3D fluid flows,'' Physica D **149**, 248–277 (2001).
Haller, G. and Yuan, G., ''Lagrangian coherent structures and mixing in two-dimensional turbulence,'' Physica D **147**, 352–370 (2000).
Lapeyre, G., personal communication (2001).
Lapeyre, G., Hua, B. L., and Legras, B., ''Comment on 'Finding finite-time invariant manifolds in two-dimensional velocity fields,' '' Chaos **11**, 427 (2001).